

Determining the radial distribution of the emission coefficient from a plasma source

C. GAVRILĂ*, I. GRUIA^a, C. P. LUNGU^b

Faculty of Building Services and Equipment, Technical University of Civil Engineering Bucharest, Romania

^a*Faculty of Physics, University of Bucharest, Romania*

^b*National Institute for Laser, Plasma and Radiation Physics*

The purpose of this paper is to determine the radial distribution of the emission coefficient from the measured intensity distribution emitted by an extended source of radiation, particularly a plasma source. The source is assumed to be optically thin and axially symmetrical. This problem is solved by inverting Abel's integral equation. A smoothing procedure is made on the experimental curve in order to attenuate the random errors before computing the derivative. The integral is calculated analytically in a small interval on the right of the discontinuity point; the other part is estimated numerically in Scilab program.

(Received June 14, 2009; accepted July 20, 2009)

Keywords: Radial distribution, Plasma source, Abel's integral equation, Scilab

1. Introduction

Abel's integral equation is frequently applied in the study of the extended radiation sources with cylindrical symmetry. A measurement of the transverse distribution $I(y)$ of the intensity emitted perpendicularly to the source axis allows the calculation of the emission coefficient radial distribution $F(r)$. If the source is optically thin, the intensity $I(y)$ is connected to the emission coefficient (Fig. 1) by the formula:

$$I(y) = \int_{-x}^x F(r) dx. \quad (1)$$

Setting $r = \sqrt{x^2 + y^2}$ and $x = \sqrt{R^2 - y^2}$ we can write

$$I(y) = 2 \int_y^R \frac{rF(r)}{\sqrt{r^2 - y^2}} dr. \quad (2)$$

$F(r)$ can be deduced from $I(y)$ by the inverse formula [1]

$$F(r) = -\frac{1}{\pi} \int_y^R \frac{dI(y)}{dy} \frac{1}{\sqrt{r^2 - y^2}} dy, \quad (3)$$

known as Abel's integral equation.

$I(y)$ and $F(r)$ need not necessarily be the transverse intensity and the local emission coefficient respectively; they can also represent other physical quantities such as the optical thickness and the absorption coefficient of a cylindrical absorbing plasma, and the optical path and the refractive index of cylindrical plasmas.

Fig. 1 illustrates the basic idea of the cross-section of plasma with the cylindrical symmetry.

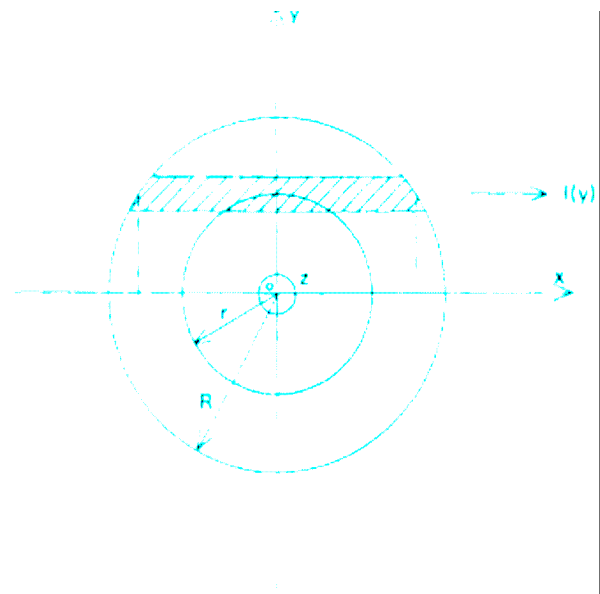


Fig. 1: Cross-section of plasma with the cylindrical symmetry.

2. Method of solution

Our method consists in computing $I(y)$ derivative using the spline function of the Scilab program, and integrating the formula (3) using the intsplin function of the same program. There is a discontinuity at $y = r$ of the integrand of the equation (3) which causes the principal computational difficulties when the integral is calculated analytically.

For the determination of $F(r)$ we have to take into consideration the errors give by the following factors:

1. Measurements made for $I(y)$ which mislead errors in the calculation for $dI(y)/dy$. In order to diminish these errors we use the method of approximation with cubic spline interpolations. In Scilab we use the function `splin` and `interp`, and for adjustment of $I(y)$ we choose `splin` with option "monotone" at exit:

```
y = linspace(0,1,12);
yi = 0 : 0.01 : 1;
size(y);
I = [1.00666650  0.998857748  0.996478771
     0.868547895  0.614427122  0.444704597
     0.360332898  0.315408616  0.297430998
     0.283713004  0.271939569  0.261930];
```

```
size(I);
```

```
d = splin(y,I,"monotone");
```

```
Ii = interp(r, y, I, d);
```

2. The integrant of formula (3) have 2 singularities:

- for $r = 0$ the integral is convergent if approximation of $dI(y)/dy$ is considered a polynomial of second degree with the form $a \cdot y^2 + b \cdot y$ (if the free term is not zero the integral is divergent).

- for $y = r$, this represents the hardship in the calculation of $F(r)$. For overcome this difficulty the expression of $F(r)$ gets this form:

$$F(r) = -\frac{1}{\pi} \left[\int_r^{r+h} \frac{dI(y)}{dy} \frac{1}{\sqrt{y^2 - r^2}} dy + \int_{r+h}^R \frac{dI(y)}{dy} \frac{1}{\sqrt{y^2 - r^2}} dy \right]$$

The first integral can be calculated using a polynomial of second degree for approximation of $dI(y)/dy$ (see 1), and the second integral was calculated using an approximate numerical method given by the function `intsplin` of the Scilab program.

The solution was obtained in Scilab, by defining the function which solves numerically the second integral.

3. Experimental, application to plasma spectroscopy (He-Ne plasma)

The plasma was produced inside a gas tube by an DC electrical discharge. (Fig 2). The gas in the tube was electrically neutral, and as long as no external energy was applied, most of the atoms were in the ground state. When the high electrical voltage was applied, electrons were released from the cathode and accelerated toward the anode. On their way these electrons collide the gas atoms and transfer energy to them. Thus, the gas atoms were raised to excited state.

High voltage was required to start the electrical discharge in the tube in order to maintain the discharge. Thus, a high voltage pulse was applied for the initial

breakdown of the discharge, and then the voltage was lowered to its operating value.

The ballast resistor was used to limit the current in the tube after the discharge breakdown. The gas mixture was 85-90% helium, and 10-15% neon. The total gas pressure was of about 10^3 Pa. At the extremities of the tube, the electrodes were attached to a high voltage power supply (DC).

For data acquisition were used two types of spectrometric equipment:

- High-resolution Spectrometer HR4000 UV/VIS: spectral range 245 nm ÷ 690 nm, resolution 0,3 nm; grating H1, installed, select 425-445 nm; installed optical bench entrance aperture, 5 μ m width;
- High-resolution Spectrometer HR4000 NIR: spectral range 685 nm ÷ 1100 nm, resolution 0,3 nm; grating H1, installed, select 425-445 nm; installed optical bench entrance aperture, 5 μ m width; Cross-platform Spectroscopy Operating Software.

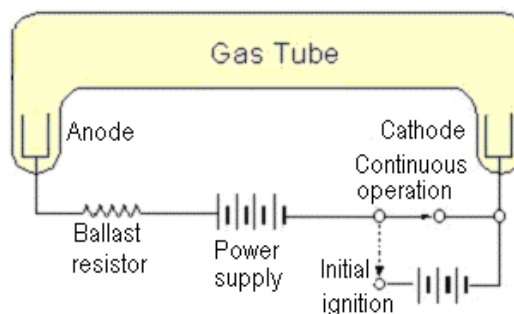


Fig. 2. Electrical excitation of a gas tube.

For the spectral acquisition was used the optical fibre QP450-2-XSR: 455 μ m Fiber, extreme solarization-resistant, 2 m length for High-resolution Spectrometer HR4000 UV/VIS and QP400-2-VIS : 400 μ m Premium Fiber, VIS/NIR, 2 m length for High-resolution Spectrometer HR4000 NIR.

Fig. 3 shows the principle scheme of the HR 4000 Spectrometer.

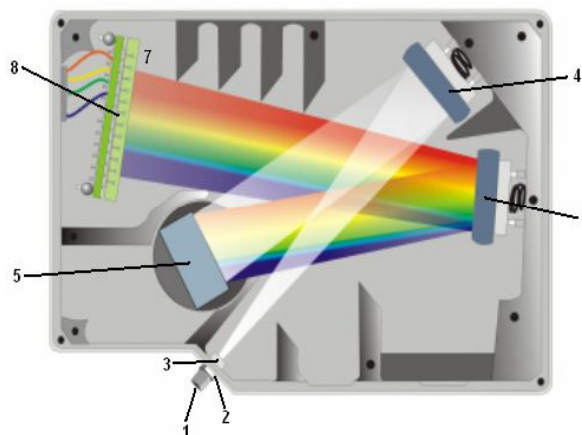


Fig. 3. The principle scheme of the HR 4000 Spectrometer; 1- SMA Connector; 2- Slit; 3- Filter; 4- Collimating Mirror; 5- Grating; 6- Focusing Mirror; 7- L2 Detector Collection Lens; 8- CCD Detector.

The spatial resolution acquisition scheme is shown in Fig. 4 for $y = 0$, $dy = dz = 0.4mm$ and $dx = 35mm$.

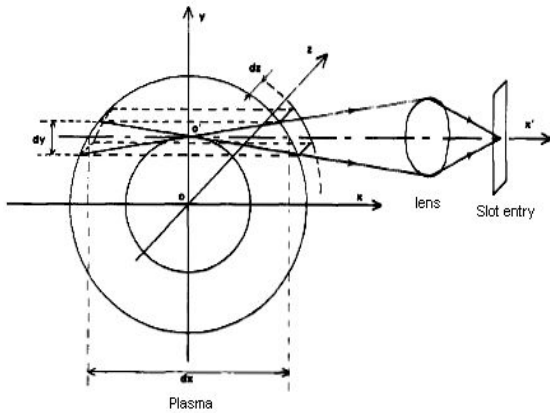


Fig. 4. The optical montage and the spatial resolution acquisition scheme of the plasma.

The values for the distribution of the acquired normalized intensity, $I(r)$, for three different wavelengths are found in the table below:

Table 1. Distribution of normalized intensity for different wavelengths.

Radial distribution for $\lambda = 587.39[nm]$	Radial distribution for $\lambda = 667.71[nm]$	Radial distribution for $\lambda = 702.51[nm]$
0.9147523	0.976853	0.6974521
0.8930498	0.8989501	0.7233099
0.8463472	0.8155697	0.7677070
0.7421716	0.7355681	0.7788591
0.654281	0.6564681	0.7651649
0.5914480	0.5785038	0.7332288
0.4989751	0.5023404	0.6881532
0.4421234	0.4287733	0.6320176
0.3683610	0.3593891	0.5680724
0.3076279	0.2946344	0.4990842
0.2491980	0.2358085	0.4268970
0.1972479	0.1829499	0.3545373
0.1507051	0.1370362	0.2837645
0.1106482	0.0976156	0.2171498
0.0765571	0.0651735	0.1564124
0.0490978	0.0391599	0.1039254
0.0278312	0.0195296	0.0605388
0.0128134	0.0058284	0.0283179
0.0035677	0.0024852	0.0072610
0.0008283	0.0014647	0.0027764
0.	0.	0.

r	I(r) for $\lambda = 587.39[nm]$	I(r) for $\lambda = 667.71[nm]$	I(r) for $\lambda = 702.51[nm]$
0.	1.	1.	1.
0.05	0.9938121	0.9928906	1.0062758
0.1	0.9752485	0.9746492	1.0140824
0.15	0.9447778	0.9452760	1.0168376
0.2	0.9030564	0.9045837	1.0107914
0.25	0.8445247	0.8529467	0.9934946
0.3	0.7899869	0.7912067	0.9632634
0.35	0.7213576	0.7209542	0.9192561
0.4	0.6467279	0.6440599	0.8614725
0.45	0.567973	0.5630496	0.7904485
0.5	0.4871554	0.4803555	0.7079443
0.55	0.4063379	0.3985033	0.6160263
0.6	0.3276767	0.3199252	0.5178325
0.65	0.2534221	0.2468662	0.4170366
0.7	0.1857304	0.1811974	0.3179244
0.75	0.1265704	0.1243218	0.2251645
0.8	0.0776299	0.0776427	0.1435788
0.85	0.0405963	0.0416277	0.0776825
0.9	0.0157510	0.0167446	0.0312261
0.95	0.0030002	0.0026193	0.0061228
1.	0.	0.	0.

4. Results and discussion

The values for the distribution of the radial intensity after calculations are presented in the table below:

Table 2. Distribution of radial intensity for different wavelengths.

In this study the model parameters were assessed based on an analysis of field experimental data with good results. Results of the analysis are presented in Figs. 5 and 6.

The plot containing the distribution of the intensity, $I(y)$, and the emission coefficient radial distribution $F(r)$ for three different wavelengths were obtained in Scilab and presented below.

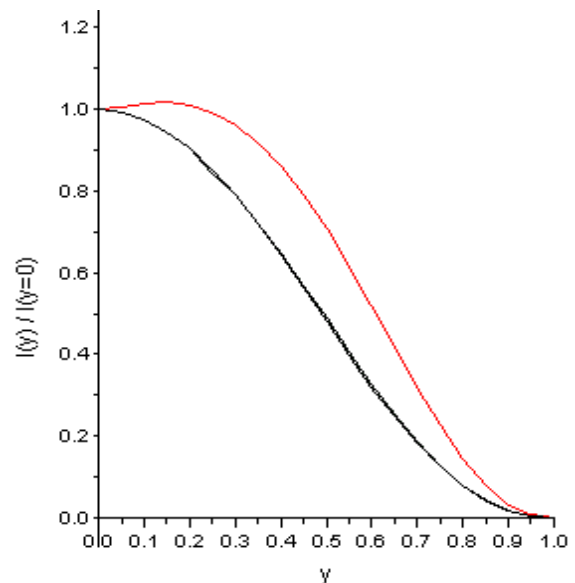


Fig. 5. The distribution of intensity for three different wavelengths.

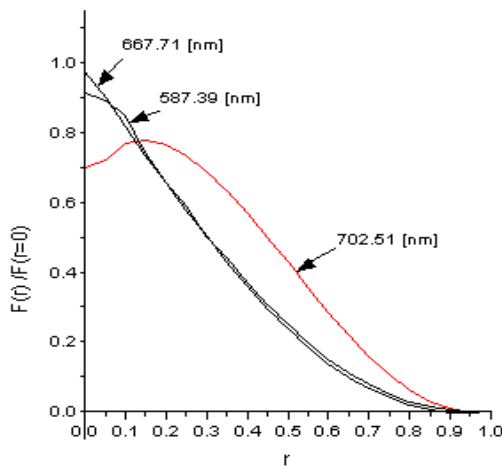


Fig. 6. The emission coefficient radial distribution $F(r)$ for three different wavelengths.

5. Conclusions

The emission coefficient radial distribution was determined from the measured intensity distribution emitted by an extended source of radiation, particularly a plasma source. The source was assumed to be optically thin and axially symmetrical. This problem was solved by inverting Abel's integral equation. A smoothing procedure was made on the experimental curve in order to attenuate the random errors before computing the derivative. The integral was calculated using a polynomial of second degree for the approximation of $dI(y)/dy$ in a small interval on the right of the discontinuity point, the other part was calculated using an approximate numerical method given by the function *intsplin* of the Scilab program.

Acknowledgements

This work was supported by National Institute for Laser, Plasma and Radiation Physics under the contract PNCDI II, 72-223/01.10.2008.

References

- [1] R. Bracewell, The Fourier transform and its applications (Mac-Graw Hill, New York), 262 (1965).
- [2] C. Gavrilă, M. R. Gavrilă, Metode numerice rezolvate în MathCad și Matlab/Scilab, 2004, Ed MATRIX ROM, ISBN 973 – 685 – 852 – 9.
- [3] R. Gorenflo, Y. Kovetz: Solution of an Abel type integral equation in the presence of noise. IPP/6/29, Institut für Plasmaphysik, Garching bei München, November 1964.
- [4] R. M. Hoffman, H. L. Pardue - Stacked spectral display for improvement of wavelength range – resolution trade off with a vidicon detector, Anal. Chemistry **51**, 1267 (1979).
- [5] H. L. Felkel, H. L. Pardue, Anal. Chemistry **49**, 11 (1977).
- [6] C. R. Fleurie, E. J. Chapell, H. R. Griem, New Phys. Comm. **7**, 200 (1974).
- [7] R. Gorenflo, Y. Kovetz, Numerische Mathematik **8**, 392 (1966).
- [8] Y. Talmi, (Ed.) Multichannel image detectors, Amer. Chem. Soc. (series 102), Washington, 1979.
- [9] I. Iova, Gh. Ilie, I. Gruia, M. Băzăvan, The Int. Society for Optical Engineering, Washington, USA, SPIE **3405**, 524 (1998).

*Corresponding author: cgavrila2003@yahoo.com